Numerical analysis of ventilated windows' thermal behaviour under summer condition

Shiva Najaf Khosravi [a], *Ardeshir* Mahdavi [a]

[a] Department of Building Physics and Building Ecology, Vienna University of Technology, Vienna, Austria, shiva.khosravi@tuwien.ac.at, amahdavi@tuwien.ac.at.

Abstract. Efforts to develop advanced building envelope components have pursued, among other things, ventilated window constructions. To properly configure ventilated windows, both the operation mode and the climatic context must be taken into consideration. In the framework of a previous research project, an instance of a ventilated window (outdoor air curtain mode) was implemented in a testbed and was subjected to experimental studies under summer conditions. In the present contribution, we numerically evaluate the thermal behavior of this system via computational fluid dynamic (CFD) simulation. Specifically, we compared simulation results with measurement data to evaluate the accuracy of the simulation model. Thereby, the main objective was to explore the fidelity of the CFD model and its potential for supporting the design of ventilated windows. To this end, the utility of the CFD was demonstrated in terms the optimization of the design of a ventilation window (exhaust and outdoor curtain mode). In the course of this study, we numerically analyzed the thermal behavior of the two modes of ventilation window operation (exhaust and outdoor curtain mode) under summer conditions. The results of the CFD-based investigation suggest that the application of low-emissivity glazing as the exterior glass pane can improve the cooling effect in both cases. In addition, the exhaust mode of the ventilated window shows a better performance under summer boundary conditions.

Keywords. Heat transfer, ventilated window, CFD simulation, energy performance.
DOI: https://doi.org/10.34641/clima.2022.370

1. Introduction

Ventilated windows have received increased attention due to their potential to contribute to indoor air quality and higher energy efficiency [1]. A ventilated window can regulate, in theory, the interaction between the outdoor and the indoor climate due to its adaptability [2]. This window is composed of a multi-layered structure. In certain instances, it includes transparent panels as an external and internal layer and a ventilated buffer space in between. Operable vents located at the top and bottom of the frames enable, depending on the operation mode, the flow of air in the cavity [3-5]. Ventilated windows can be employed in many regions with various climate conditions [3, 6, 7]. Generally speaking, five main operation modes of a ventilated window can be distinguished, namely i) supply, ii) exhaust, iii) indoor air curtain, iv) outdoor air curtain and v) insulation mode. To properly configure ventilated windows, both the operation mode and the climatic context must be taken into consideration [3].

As the name implies, the main distinction between conventional windows and ventilated windows is the presence of free or forced convection in the interstitial cavity between the window's layers [8]. A ventilated window functions as a solar collector under incident solar radiation. The solar energy passing through the outer glazing warms up the interstitial space and eventually internal glazing surfaces. Re-emitting the trapped heat from these surfaces increases the indoor air temperature. Hence, the thermal behavior of ventilated windows strongly affects the indoor temperature and consequently energy consumption of a building [3].

Predicting the thermal behavior of a ventilated window is not a trivial task. Temperature and airflow patterns evolve due to various dynamic and interdependent thermal and aerodynamic processes. These processes depend on weather conditions, geometry, thermophysical properties of the several constituent components of the ventilated window structure, and the building itself [9-11]. Detailed numerical modeling of ventilated windows to address the full complexity of these systems necessitates the combined representation of heat, mass, and momentum transfer [12]. Modeling and simulation of fluid dynamics in such a system require a high degree of accuracy in details to obtain a high

degree of fidelity toward representation of the reality [4]. As many studies have confirmed, The numerical model (for example, CFD simulations) has the potential to yield a full-scale domain with a complicated boundary layer such as an inner layer, including the thin viscous sublayer or the buffer layer [13]. The numeric analysis of the thermal behavior of ventilated windows has received significant attention in the literature in the last few decades [3, 8, 10, 14-17]. Nevertheless, various approaches to the modeling of heat transfer phenomena in the ventilated windows are seen with a different level of accuracy, depending on the overall goal of the modeling project [4]. For instance, deployment of purely two-dimensional CFD models may be considered as less than ideal [10, 18-20].

In some studies, the dependency of material-related properties on temperature is not considered [10, 20-22]. Likewise, the influence of solar radiation is not included in a number of studies [18, 21, 22]. Most CFD studies model the thermal performance of the window under the assumption of a constant outdoor temperature and do not consider the wind impact. In some cases [16, 23-25], heat transfer coefficients for indoor and outdoor surfaces are considered. These observations imply that, despite significant progress in the CFD-supported study of ventilated windows, the intricate nature of heat transfer and airflow within a ventilated window is far from being fully understood. Therefore, further research in this field is necessary.

The present contribution concerns the thermal performance of an outdoor curtain mode and exhaust ventilated window. This was done by numerically modeling the fluid dynamic and heat transfer in the window and solving the model in a commercially available CFD code. Moreover, available measured data obtained from an exprimental method was applied to evaluate the accuracy of the CFD model. The CFD model was subsequently utilized to compute air temperature, and air velocity distributions. The aim thereby was to cmpare the thermal performance of the two aforementioned ventilated windows in the summer boundary condition.

2. Method

In order to simulate the thermal behavior of the ventilated window, a CFD model was implemented in the finite volume code ANSYS FLUENT 19.0 [26]. The model involves the ventilated window mounted in the façade of a test space. Ansys design modeler and Ansys meshing were applied as a pre-processor to create the geometry, mesh, and the computational domain. In this model, a mesh with hexahedral element was generated. To achieve higher resolution concerning the air movement in the cavity, a finer mesh was applied between the glass sheets. The grid cell size within the cavity was kept to a maximum of 2 mm, as larger dimensions would significantly alter the results. A grid independence study has been performed to ensure the adequacy of the mesh density. Due to the transient outdoor boundary condition, the thermal behavior of the glazing units is rather dynamic. However, due to their relatively small thermal mass, the glazing units react realtively swiftly to the dynamics of prevailing thermal conditions. Based on this observation and considering the computational cost, the thermal processes in the ventilated window were modeled as steady-state mode [27].

In the present study a three-dimensional domain in a steady-state mode was applied. The conservation equation for mass, momentum, and thermal energy, which is known as Reynolds-averaged Navier–Stokes equation was solved to predict the field variables temperature and velocity. The corresponding partial differential equations for continuity (1), momentum (2), and energy (3) are as follows [28]:

$$\frac{\partial}{\partial t}\left(\int_V \rho dV\right) + \oint_A \rho V_r . da = 0 \quad (1)$$

$$\frac{\partial}{\partial t}\left(\int_V \rho dV\right) + \oint_A \rho v_r \otimes v . da = -\oint_A pI . da + \oint_V f_b \, dV \quad (2)$$

$$\frac{\partial}{\partial t}\int_V \rho E dV \oint_A [\rho H V_r + v_g p]. \mathrm{da} = -\oint_A q". da + \oint_A T . vdA + \oint_V f_b . vdV + \oint_V S_E \, dV \quad (3)$$

Thereby, v presents continuum velocity, v_r is the relative velocity; V is volume; a is the area; p is the pressure; I is the unit vector; T presents the viscous stress tensor; E is the total energy; H is the enthalpy; $q"$ is the heat flux vector; $\otimes$ is kronecker product; S_E radiation energy source.

Buoyancy due to density change was applied in the energy equation. The discrete ordinates (DO) model was applied as the radiation model [29, 30]. This model is capable of modelling glass, a semi-transparent medium [10]. The widely deployed K-ε realizable turbulence model was applied [3, 8, 31, 32]. The pressure based solver was used [17].

For pressure–velocity coupling, the SIMPLE segregated solver was applied[17]. The discretization scheme used for the momentum, energy, turbulent kinetic energy, and specific dissipation rate was the second order upwind scheme. Pressure Staggering Option (PRESTO) was used for the pressure discretization scheme. Gradient reconstruction was done using The Least Squares Cell-based method [17]. The acceptable residual limits were set at $<10^{-3}$ for continuity, x, y and z momentum, turbulent kinetic energy and turbulent specific dissipation, whereas this limit for energy was $<10^{-6}$ [3, 17]. Monitors for area weighted static temperature on the supply vent, maximum velocity in the cavity area and supply vent mass flow rate were setup. Three types of materials were applied in each simulation, namely transparent fluid (air), semi-transparent solids (glazing), and opaque solids (frames and walls). Table 1 summarizes the assumed physical properties of the layers.

As mentioned earlier, in the course of this study, we

numerically analyzed the thermal performance of the two modes of ventilation window operation (exhaust and outdoor curtain mode) under summer conditions. Figure 1 schematically illustrates the vertical section of the ventilated window for the summer case.

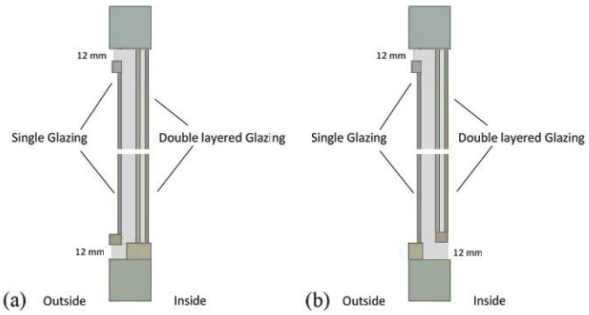

Fig. 1 - Schematic illustration of ventilated window for the summer case; a: outdoor curtain mode, b: exhaust.

Tab. 1 - Assumed properties of simulated glazing units.

	Single glazing (6 mm)	Low-Emissivity double glazing (4+12+4 mm)
Transmittance	0.752	0.305
Reflectance	0.143	0.402
Absorbance	0.105	0.250
Emissivity	0.84	0.148
Thermal conductivity [$W.m^{-1}.K^{-1}$]	1	0.043

2.1 Comparison with measurements

To evaluate the CFD model's reliability, a reference case (outdoor curtain mode) corresponds to the actually implemented experimental setup [33]. During the field trial, the thermal performance of the ventilated window and the effect of solar radiation were evaluated under real outdoor climate conditions [33]. The location of the field trial was Stetten, Austria (Latitude: 48°14'N; Longitude: 16°21'E). A 1.2 m wide and 2.1 m high ventilated window was installed in the Holzforschung test facility [33]. One side of the window was exposed to real weather condition and the other side faced a thermally conditioned room. The measurement accuracy of the air temperature sensors and thermocouples were ± 0.1 K and ± 1.5 K respectively [33]. According to the experimental results, the wind effect was not noteworthy. On the other hand, the solar radiation showed a visible difference in the temperature conditions in the buffer area. During the night, the temperature at the lower measuring position was derived by the outside air temperature. The air temperature at the upper opening was about 5 K higher than at the lower measuring point. On the other hand, during the daytime, the effect of solar radiations was more obvious since the maximum temperature difference between top and bottom opening was about 20-30 K [33]. In this study, a one-hour long segment of measured data from the third day of measurements could be identified as involving relatively small fluctuations of the boundary conditions. We thus could treat this period as quasi steady-state. The registered mean values of the boundary condition during this one-hour period (10:00 AM, July 16th, 2016) were treated as the applicable boundary conditions for the CFD simulation model. Table 2 shows the boundary condition for the summer case.

Tab. 2 - Boundary condition for the CFD simulation.

Variable	Value	Unit
Irradiation	650	$W \cdot m^{-2}$
Wind Speed	2	$m.s^{-1}$
Outdoor Temperature	22	°C
Indoor Temperature	25	°C

Figure 2 illustrates the temperature distribution profile (along the depicted path) obtained from the CFD simulation together with the measured temperature at two sensor locations in the window specimen.

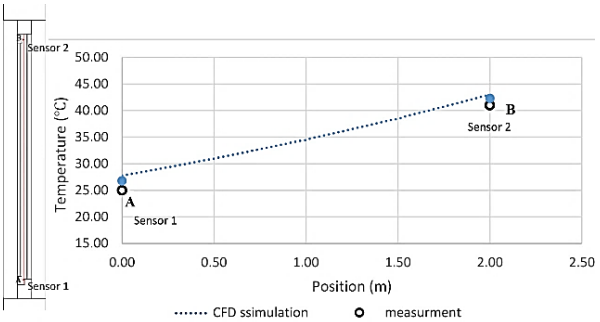

Fig. 2 - Left: schematic section through the examined ventilated window with the position of the two temperature probes; Right: Measured (sensors A and B) and simulated temperature profile. The x-axis denotes the relative distance.

The measurement results reported the effect of solar radiation on warming the air temperature in the interstitial space during the warm season. The CFD simulation slightly overestimates the temperature values. However, simulation results may be suggested to agree in tendency with the measurements.

3. Thermal behavior of exhaust and outdoor curtain ventilated window

As mentioned earlier, one of the goals of this study was to computationally investigate the thermal behavior of ventilated window (exhaust and outdoor curtain mode) during the warm season. To this end, the thermal behavior of two modes of ventilated windows under the identical boundary conditions

and identical dimensions (1 m wide and 1 m high) were estimated. According to the results, in both cases, the temperature difference among openings at the top and bottom opening was between 12-20 K. For the sake of comparison, Figure 3 demonstrates temperature and velocity counters for exhaust (a, b) and outdoor curtain air (c, d) ventilated windows.

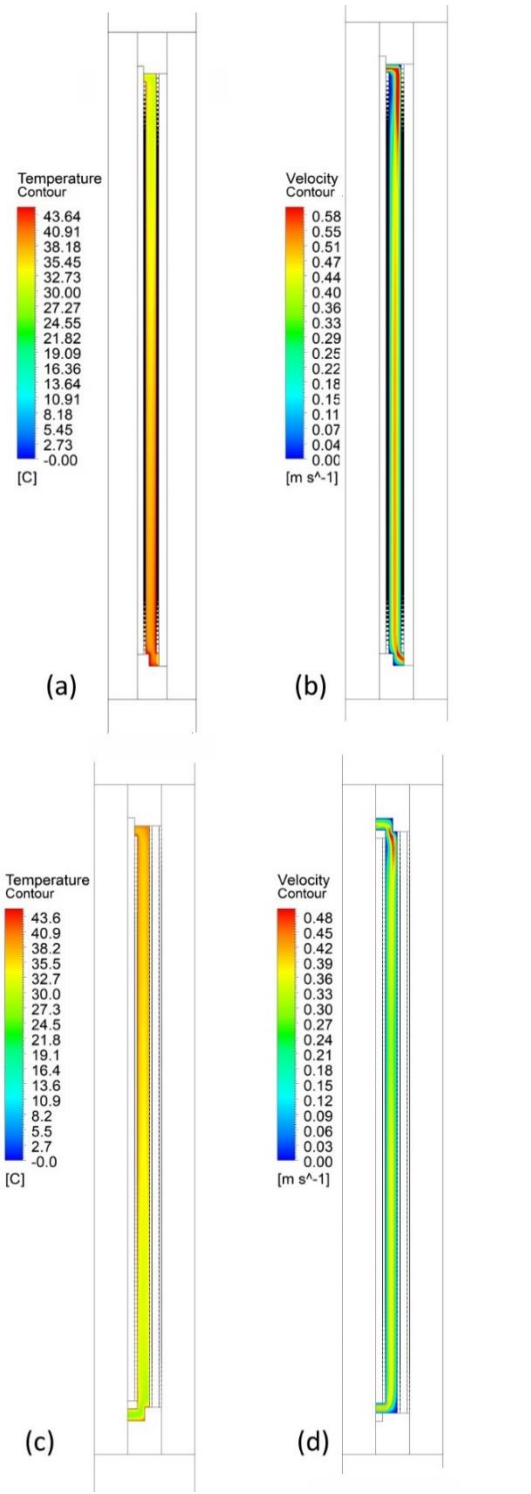

Fig. 3 - Temperature and velocity distribution in the window cavity, a,b: exhaust and b,c curtain air ventilated window.

In the exhaust air ventilated window the mean air temperature and consequently the air velocity is higher. In this type of the ventilated window the buffer space is connected to the indoor air temperature. The solar radiation heats the outside surface of the glass to induce airflow out of the indoor space. The generated negative pressure makes the outdoor fresh air enter from other openings of the room. The system is appropriate when the outdoor temperature is not so high. On the other hand, the Curtain air window expels the accumulated warm air from the buffer space. The solar radiation induces airflow in the interstitial space and consequently reduces heat flux into the room through the glass. This type of the window could represent a proper option for the warm season.

To assess the effect of double-layered glazing location, four cases were considered as per Table 3. The assumed window dimensions are identical in all four cases (1 m wide and high).

Tab. 3 - Summary of the simulated configurations (width of the inlet and outlet opening was assumed to be 12 mm in all cases).

Case	Ventilated window type	Position of the double-layered element
A	outdoor curtain	inside
B	outdoor curtain	outside
C	exhaust	inside
D	exhaust	outside

In order to reduce energy consumption and improve the indoor thermal environment of the buildings, the mean temperature, mean velocity, and inner layer glazing temperature should be considered. Table 4 summarizes the simulation results for the four cases in terms of the mean temperature of the inner layer glazing and buffer space.

Tab. 4 - Temperature difference, mean air velocity and man surface temperature for the simulated scenarios.

Case	Mean temperature (°C)	Mean velocity ($m.s^{-1}$)	Inner layer glazing temperature (°C)
A	34.0	0.31	38.3
B	32.9	0.30	32.5
C	36.2	0.43	41.4
D	34.4	0.41	36.8

The results of the CFD-based investigation suggest that the application of low-emissivity glazing as the exterior glass pane can improve the cooling effect in both cases. According to the results, with help of low-emissivity glazing as the exterior pane, the surface temperature of the interior glass drops, and

consequently, the radiation exchange between this surface and the occupants can be decreased. In addition, the outdoor curtain air mode of the ventilated window reveals a slightly better performance under summer boundary conditions by reducing the temperature difference between the room air and the surface of the interior glass.

4. Conclusion

The present study entailed the thermal analysis of several ventilated window configurations. The thermal performance of the corresponding models was evaluated for summer boundary conditions numerically by a commercially available CFD tool. As remarked at the outset of the paper, the deployment of numerical methods in heat transfer simulation of building details requires careful attention to issues such as the details of the model, mesh generation, and boundary conditions.

To gain confidence concerning the model's reliability, its performance was first compared with field measurement results. The thermal performance of the ventilated windows was assessed in view of four criteria, namely: i) mean air temperature of the interstitial space, ii) mean flow velocity in the cavity, iii) inner layer glazing temperature, iv) The temperature difference between the buffer area and outdoor zone.

Analysing the summer performance of two types of ventilated windows (exhaust and outdoor curtain mode) revealed that the application of low-emissivity glazing as the exterior glass pane can improve the cooling effect in both cases. In addition, the outdoor curtain air mode of the ventilated window displayed a more efficient performance under summer boundary conditions. On the other hand, the operation of the exhaust mode window during periods of milder outdoor conditions lowers the room air pressure. Hence, air may flow into the room from adjacent spaces air via openings and cracks.

Future studies are required to both empirically and computationally determine the annual energy saving potential related to the use of ventilated windows. These investigations would have also to address the monetary and environmental implications regarding the production, installation, and maintenance of ventilated windows.

5. Acknowledgment

The authors gratefully acknowledge Dr. Julia Bachinger of the Holzforschung Austria for the provision of the empirical testing data used in this paper.

6. References

[1] He G, Shu L, Zhang S. Double skin facades in the hot summer and cold winter zone in China: Cavity open or closed? Building Simulation. 2011;4(4):283-91.

[2] Ahmed M, Abdel-Rahman A, Ali PDEAHH, Suzuki M. Double Skin Façade: The State of Art on Building Energy Efficiency. Journal of Clean Energy Technologies. 2016;4:84-9.

[3] Najaf Khosravi S, Mahdavi A. A CFD-Based Parametric Thermal Performance Analysis of Supply Air Ventilated Windows. Energies. 2021;14(9).

[4] Jankovic A, Goia F. Impact of double skin facade constructional features on heat transfer and fluid dynamic behaviour. Building and Environment. 2021;196:107796.

[5] Oesterle E, Lieb R.-D, Lutz M, Heusler W. Double-skin Facades : Integrated Planning. München: Prestel; 2001.

[6] Xu L, Ojima T. Field experiments on natural energy utilization in a residential house with a double skin façade system. Building and Environment. 2007;42:2014-23.

[7] Hien WN, Liping W, Chandra AN, Pandey AR, Xiaolin W. Effects of double glazed facade on energy consumption, thermal comfort and condensation for a typical office building in Singapore. Energy and Buildings. 2005;37:563-72.

[8] Najaf Khosravi S, Mahdavi A. Simulation support for the design of ventilated windows: a case study. Building Simulation 2021; Bruges, Belgium. 2021.

[9] Hensen J, Barták, M, Frantisek D. Modeling and simulation of a double-skin façade system. ASHRAE Transactions. 2002;108(2):1251-9.

[10] Gosselin JR, Chen Q. A computational method for calculating heat transfer and airflow through a dual-airflow window. Energy and Buildings. 2008;40(4):452-8.

[11] Jiru TE, Haghighat F. Modeling ventilated double skin façade—A zonal approach. Energy and Buildings. 2008;40(8):1567-76.

[12] Gavan V, Woloszyn M, Kuznik F, Roux J-J. Experimental study of a mechanically ventilated double-skin façade with Venetian sun-shading device: a full-scale investigation in controlled environment,. Sol Energy. 2010; 84 (2):183–95.

[13] Wilcox D.C. Turbulence modelling for CFD. . DCW Industries1998.

[14] Tanimoto J, Kimura K-i. Simulation study on an air flow window system with an integrated roll screen. Energy and Buildings. 1997;26(3):317-25.

[15] Saelens D, Roels S, Hens H. The inlet temperature as a boundary condition for multiple-skin facade modelling. Energy and Buildings. 2004;36(8):825-35.

[16] Bhamjee M, Nurick A, Madyira DM. An experimentally validated mathematical and CFD model of a supply air window: Forced and natural flow. Energy and Buildings. 2013;57:289-301.

[17] Bhamjee M. A computational fluid dynamics and experimental investigation of an airflow window. Johannesburg, South Africa: University of Johannesburg; 2011.

[18] McEvoy ME, Southall RG, Baker PH. Test cell evaluation of supply air windows to characterise their optimum performance and its verification by the use of modelling techniques. Energy and Buildings. 2003;35(10):1009-20.

[19] Southall R, McEvoy M. Investigations into the functioning of a supply air window in relation to solar energy as determined by experiment and simulation. Solar Energy - SOLAR ENERG. 2006;80:512-23.

[20] Xu X-l, Yang Z. Natural ventilation in the double skin facade with venetian blind. Energy and Buildings. 2008;40(8):1498-504.

[21] Southall R, McEvoy M. Results From a Validated CFD Simulation of a Supply Air 'Ventilated Window'. Air Distribution in Rooms (ROOMVENT). 2000;2:1049-54.

[22] Safer N, Woloszyn M, Roux JJ. Three-dimensional simulation with a CFD tool of the airflow phenomena in single floor double-skin facade equipped with a venetian blind. Solar Energy. 2005;79(2):193-203.

[23]Gloriant F, Tittelein P, Joulin A, Lassue S. Modeling a triple-glazed supply-air window. Building and Environment. 2015;84:1-9.

[24]Parra J, Guardo A, Egusquiza E, Alavedra P. Thermal Performance of Ventilated Double Skin Façades with Venetian Blinds. Energies 2015;8(6):4882-98.

[25] Wang E, Wang H, Deng M, Wang K, Wang Y. Simulation of the ventilation and energy performance of a PV-integrated breathing window. Procedia Engineering. 2017;205:2779-84.

[26] Fluent 19.0, 2018, User's Guide. fluent Inc., Lebanon.

[27] Skaff MC, Gosselin L. Summer performance of ventilated windows with absorbing or smart glazings. Solar Energy. 2014;105:2-13.

[28] Cho, K.-j., Cho, D.-w. Solar Heat Gain Coefficient Analysis of a Slim-Type Double Skin Window System: Using an Experimental and a Simulation Method. Energies. 2018, *11*,1-15.

[29] Torre ATdl, Abel E, Saelens D, Carmeliet J, M. Baelmans. Investigation on airflow and heat transfer of a glazing facade with external louvers 4th International Building Physics Conference; Istanbul2009.

[30] Choudhary R, Malkawi A. A methodology for micro-level building thermal analysis: combining CFD and experimental set-ups. Seventh International IBPSA Conference. 2001:1275-82.

[31] Pasut W, De Carli M. Evaluation of various CFD modelling strategies in predicting airflow and temperature in a naturally ventilated double skin façade. Applied Thermal Engineering. 2012;37:267-74

[32] Launder B, Spalding DB. The Numerical Computation of Turbulent Flow Computer Methods. Computer Methods in Applied Mechanics and Engineering. 1974;3:269-89

[33] Nusser, B.; Bachinger, J.; Schober, K.P. Untersuchungen zur hygrothermischen Funktionsweise des low-tech Window Air Verbundfensters. Holz Forschung Austria, Vienna, 2016.

Data Statement

Data sharing not applicable to this article as no datasets were generates or analysed during the current study.